Chemistry & Biology
Article

Bacterial and Eukaryotic Phenylalanyl-tRNA Synthetases Catalyze Misaminoacylation of $tRNA^{Phe}$ with 3,4-Dihydroxy-L-Phenylalanine

Nina Moor,[1] Liron Klipcan,[2] and Mark G. Safro[2,*]
[1]Institute of Chemical Biology and Fundamental Medicine, 630090 Novosibirsk, Russia
[2]Department of Structural Biology, Weizmann Institute of Science, 76100 Rehovot, Israel
*Correspondence: mark.safro@weizmann.ac.il
DOI 10.1016/j.chembiol.2011.08.008

SUMMARY

Aminoacyl-tRNA synthetases exert control over the accuracy of translation by selective pairing the correct amino acids with their cognate tRNAs, and proofreading the misacylated products. Here we show that three existing, structurally different phenylalanyl-tRNA synthetases-human mitochondrial (*Hsmt*PheRS), human cytoplasmic (*Hsct*PheRS), and eubacterial from *Thermus thermophilus* (*Tt*PheRS), catalyze mischarging of $tRNA^{Phe}$ with an oxidized analog of tyrosine-L-dopa. The lowest level of L-dopa discrimination over the cognate amino acid, exhibited by *Hsmt*PheRS, is comparable to that of tyrosyl-tRNA synthetase. *Hsmt*PheRS and *Tt*PheRS complexes with L-dopa revealed in the active sites an electron density shaping this ligand. *Hsct*PheRS and *Tt*PheRS possessing editing activity are capable of hydrolyzing the exogenous L-dopa-$tRNA^{Phe}$ as efficiently as Tyr-$tRNA^{Phe}$. However, editing activity of PheRS does not guarantee reduction of the aminoacylation error rate to escape misincorporation of L-dopa into polypeptide chains.

INTRODUCTION

The aminoacyl-tRNA synthetases (aaRSs) play a crucial role in faithful translation of the genetic code, catalyzing selective attachment of the correct amino acid to its cognate tRNA. Covalent linkage is carried out through a two-step aminoacylation reaction, where the amino acid is first activated in the presence of ATP by formation of the aminoacyl-adenylate intermediate. The aminoacyl moiety is then transferred from AMP to the 3′-terminal ribose of tRNA, leading to the synthesis of aminoacyl-tRNA (aa-tRNA). For some aaRSs, the aminoacylation active site is unable to strictly select the cognate amino acid, rejecting others that have similar chemical structure. To maintain the accuracy of protein biosynthesis, certain aaRSs have developed the ability to hydrolyze the incorrectly aminoacylated tRNA in the specific editing site (Hendrickson et al., 2004). Prokaryotic and cytoplasmic eukaryotic phenylalanyl-tRNA synthetases (PheRSs) functioning as $(\alpha\beta)_2$ heterotetramers are capable of misactivating tyrosine, and specifically hydrolyzing the misacylated Tyr-$tRNA^{Phe}$ (Kotik-Kogan et al., 2005; Roy et al., 2004). The monomeric mitochondrial PheRSs are deprived of structural module associated with editing activity, and as a consequence catalyze stable mischarging of $tRNA^{Phe}$ with Tyr (Klipcan et al., 2009; Roy et al., 2005).

Recently we have shown that eukaryotic cells may specifically incorporate *m*-tyrosine, a product of hydroxyl radical attack on phenylalanine, via tRNA dependent pathway, utilizing mitochondrial PheRS and to a lesser extent cytoplasmic PheRS, which discriminates more efficiently between the cognate (Phe) and noncognate (*m*-Tyr) amino acids (Klipcan et al., 2009). Modification of L-tyrosine by reactive oxygen species (ROS) generates 3,4-dihydroxy-L-phenylalanine known as levodopa or L-dopa (Rodgers and Dean, 2000). Unlike *m*-tyrosine, L-dopa is a reactive species capable of further modification due to initiation of redox cycles in the presence of cellular oxidants (Rodgers and Dean, 2000). Protein-bound L-dopa is one of the most abundant modifications of proteins detected in age-related diseases; L-dopa containing proteins form protein aggregates and are inefficiently degraded by cells (Rodgers and Dean, 2000). It has been shown, using both cultured mammalian cells and a cell-free protein expression system, that L-dopa is readily incorporated into proteins, replacing tyrosine residues (Ozawa et al., 2005; Rodgers and Shiozawa, 2008). L-dopa is the most widely used treatment for Parkinson's disease, and its biosynthetic incorporation in vivo has been proposed to contribute to the disease pathology (Rodgers and Shiozawa, 2008). Being a redox-active amino acid and a selective crosslinking agent (Burdine et al., 2004), L-dopa can be genetically incorporated into proteins, using an engineered tRNA-TyrRS pair (Alfonta et al., 2003; Umeda et al., 2009). This feature facilitates the study of electron transfer in proteins, and enables structural and functional analysis of protein-protein interactions.

Here, we aimed to further study discrimination of ROS-damaged amino acids by three structurally different wild-type forms of PheRS. The kinetic data revealed that both the human mitochondrial (*Hsmt*PheRS) and cytoplasmic PheRSs (*Hsct*PheRS), and the bacterial counterpart from *Thermus thermophilus* (*Tt*PheRS) catalyze mischarging of $tRNA^{Phe}$ with L-dopa. Binding of L-dopa within the aminoacylation and editing active sites of the *Tt*PheRS and *Hsmt*PheRS crystal complexes was detected at difference Fourier maps with coefficients (F_{obs}-F_{calc}). *Hsct*PheRS and *Tt*PheRS were shown to hydrolyze L-dopa-$tRNA^{Phe}$ as efficiently as Tyr-$tRNA^{Phe}$ by *trans*-editing

Table 1. X-Ray Data Collection and Refinement Statistics for *Hsmt*PheRS and *Tt*PheRS

	*Hsmt*PheRS	*Tt*PheRS
Resolution (Å)	48.0–2.2	32.0–2.8
Space group	$P2_12_12_1$	$P3_221$
Unit cell parameters	a = 55.2 Å b = 90.6 Å c = 96.1 Å α = β = γ = 90	a = b = 173.3 Å c = 139.2 Å α = β = 90, γ = 120
R_{work}/R_{free}	17/22	23/29
Number of reflections	24,066	51,066
Completeness for range	96%	91%
Test size	5% (1236)	5% (2590)
Number of atoms	3689	8670
Rmsd bond lengths (Å)	0.007	0.008
Rmsd bond angles (°)	0.98	1.24

Rmsd, root-mean-square deviation.

activity. The data provide first evidence that L-dopa has potential to be biosynthetically incorporated into proteins in various organisms by PheRS-mediated pathways.

RESULTS

Structural Basis of Molecular Recognition of L-Dopa by PheRS

To provide the structural basis of binding and discrimination of L-dopa by PheRS, the crystal structures of *Hsmt*PheRS and *Tt*PheRS complexes with the noncognate amino acid have been determined at resolution 2.2 Å and 2.8 Å, respectively (Table 1). Analysis of the unbiased difference (F_{obs}-F_{calc}) electron density maps highlighted the electron densities that may be unambiguously attributed to the L-dopa molecules located at the amino acid-binding pockets of the aminoacylation active sites of both enzymes (Figure 1A). The electron density shaped by L-dopa differs significantly from those shaped by Phe, Tyr, or *m*-Tyr (Klipcan et al., 2009; Kotik-Kogan et al., 2005; Reshetnikova et al., 1999). Specific binding of L-dopa by PheRSs is achieved through the interactions of the phenyl ring of the ligand with the phenyl rings of two phenylalanine residues located in the so-called "FPF loop" (Phe232 and Phe234 in *Hsmt*PheRS; Pheα258 and Pheα260 in *Tt*PheRS). Three phenyl moieties thereby form a "network" of interactions, such that each aromatic pair makes an "edge-to-face" contact (Fishman et al., 2001). The anchoring of the α-NH_3^+ group of L-dopa is achieved by its interactions with the O^{γ} atom of Ser121 (Serα180 in *Tt*PheRS) and with a well-ordered water molecule, S33 (X9 in the native *Hsmt*PheRS structure; Protein Data Bank [PDB] code 3CMQ). The water molecule has been located reliably, because it was independently observed (i.e., was not included in the starting model) in almost all PheRS complexes with various ligands, occupying nearly the same positions, and is of crucial importance in hydrogen bonding coordination within the aminoacylation active site. S33 in *Hsmt*Phe*RS* is located at H bonding distances from O^{γ} of Ser121 (Serα180 in *Tt*PheRS), from $O^{\varepsilon 1}$ of Gln157 and from $O^{\varepsilon 1}$ of Glu159 (Glnα218 and Gluα220 respectively in *Tt*PheRS). One of the carboxylate oxygen atoms (O1) of the ligand forms H bonds with the side chains of Gln157 and class II invariant Arg143 (Glnα218 and Argα204 in *Tt*PheRS). All the interactions described above are common to L-dopa, Phe and other noncognate substrates (Tyr, *m*-Tyr). Compared with the cognate Phe substrate, L-dopa is additionally stabilized by the hydrogen bonding of its OH group in the *meta*-position with the $N^{\varepsilon 2}$ atom of Gln124 and the $O^{\varepsilon 2}$ atom of Glu159 (Glnα183 and Gluα220 in *Tt*PheRS). The orientation of L-dopa in the binding pocket of both *Hsmt*Phe*RS* and *Tt*PheRS is similar to that of the cognate amino acid substrate.

Misaminoacylation of tRNA^{Phe} with L-Dopa

To examine whether L-dopa is a substrate of PheRSs, we studied the ability of wild-type eukaryotic (*Hsct*PheRS and

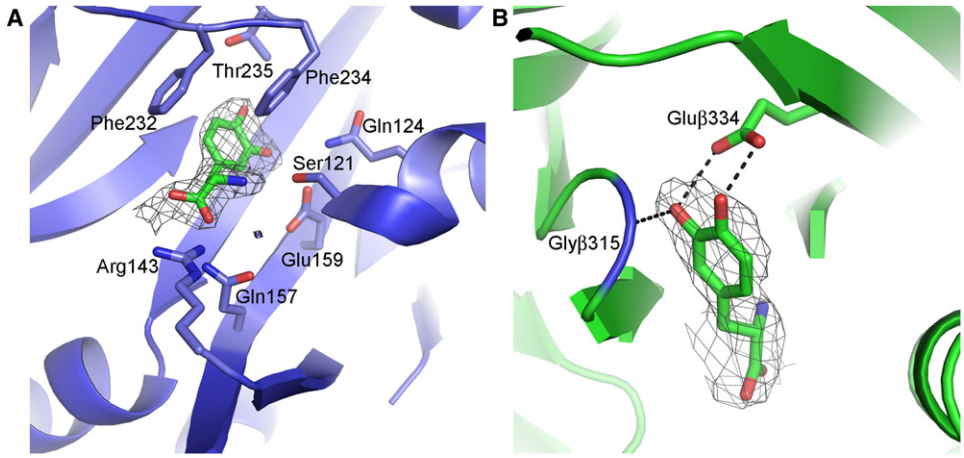

Figure 1. Binding of L-Dopa in the Synthetic and Editing Site of PheRS

(A) The aminoacylation active site of *Hsmt*PheRS (blue) in complex with L-dopa (green). The water molecule is depicted by asterisk.

(B) The editing site of *Tt*PheRS with bound L-dopa. The protein residues participating in hydrogen bonding with the OH-groups of L-dopa are shown. The electron density maps for bound ligand are contoured at 2.5 σ.

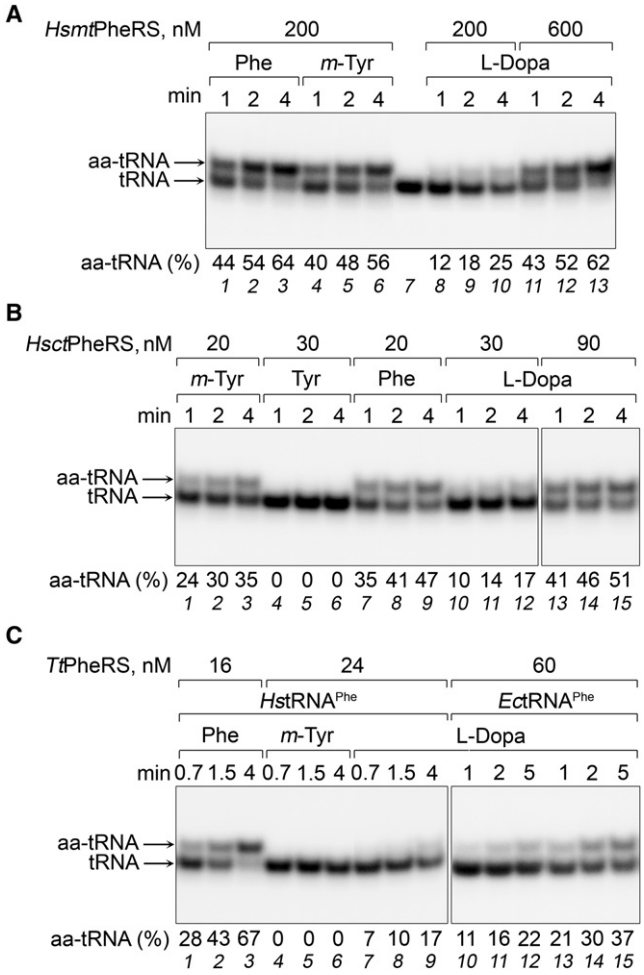

Figure 2. Aminoacylation of tRNA^{Phe} with Cognate and Noncognate Amino Acids Catalyzed by Eukaryotic and Bacterial PheRSs

(A–C) The extent of tRNA^{Phe} aminoacylation (analyzed by electrophoresis in 8% denaturing gel at acidic conditions) by (A) *Hsmt*PheRS, (B) *Hsct*PheRS, and (C) *Tt*PheRS. The aminoacylation of 2 μM *Hs*tRNA^{Phe} (A–C, lanes 1–9) or 2 μM *Ec*tRNA^{Phe} (C, lanes 10–15) was performed with 100 μM Phe, 1 mM *m*-Tyr, 1 mM Tyr, or varied L-dopa concentrations [300 μM (C, lanes 10–12) or 1 mM (the other experiments)] in the presence of indicated enzyme concentrations. Gels are representative images from three independent experiments.

*Hsmt*PheRS) and bacterial PheRSs (*Tt*PheRS) to attach this noncognate amino acid to tRNA^{Phe}. Kinetic measurements of the aminoacylation assayed by means of acidic gel electrophoresis revealed that ^{32}P-labeled human cytoplasmic tRNA^{Phe}-transcript (*Hs*tRNA^{Phe}) is mischarged with L-dopa by both the mitochondrial (monomeric) and cytoplasmic (heterotetrameric) forms of human PheRS (Figures 2A and 2B). These experiments performed in parallel with three noncognate substrates show that effective editing activity of *Hsct*PheRS preventing accumulation of the mischarged product is specifically directed against the standard amino acid, *p*-tyrosine (Tyr), but not against the ROS-damaged analogs of Phe and Tyr, *m*-Tyr and L-dopa. Using human tRNA^{Phe}-transcript, whose aminoacylated form is well separated from the free tRNA (in contrast to the respective forms of yeast tRNA^{Phe}-transcript used in our previous work) (Klipcan et al., 2009), we were able to quantify the extent of charging and to determine the kinetic parameters of the aminoacylation reactions (Table 2). Their analysis shows that the catalytic efficiency (k_{cat}/K_m) of L-dopa attachment by two human PheRSs is significantly (300-fold for *Hsmt*PheRS and 770-fold for *Hsct*PheRS) lower than that of the correct amino acid, primarily because of higher K_m values. Of two ROS-damaged amino acids tested, *m*-Tyr is the best noncognate substrate of two eukaryotic enzymes. The effectiveness of discrimination between *m*-Tyr and Phe at the level of aminoacylation is one order of magnitude higher for *Hsct*PheRS than for *Hsmt*PheRS: the respective k_{cat}/K_m values of misaminoacylation are 50-fold and 5-fold lower as compared to those of the phenylalanylation reaction. Thus, the kinetic data of the present study finally show the prevailing role of *Hsmt*PheRS in incorporation of *m*-Tyr into eukaryotic proteins, as has been hypothesized (Klipcan et al., 2009).

Mischarging of tRNA^{Phe} with L-dopa was also detected in the presence of *Tt*PheRS (Figure 2C). The experiments were performed by using two heterologous tRNA^{Phe}-transcripts (human and *Escherichia coli*, *Hs* and *Ec*) that are efficiently phenylalanylated by the bacterial PheRS at different optimal concentrations of magnesium ions (Vasil'eva et al., 2002). *m*-Tyr cannot be stably attached to either *Hs*tRNA^{Phe} (Figure 2C) or *Ec*tRNA^{Phe} (Klipcan et al., 2009). These data indicate that editing activity of *Tt*PheRS against *m*-Tyr-tRNA^{Phe} (detected previously) does not depend on the nature of tRNA^{Phe}. Comparison of relative k_{cat}/K_m values for three PheRSs (Table 2) shows that *Tt*PheRS most efficiently discriminates between L-dopa and Phe: the catalytic efficiency of L-dopa attachment by the bacterial PheRS is 1500-fold lower than that of the cognate substrate. The distinction between three enzymes in the discrimination efficiencies results mainly from differences at the level of the rate constants: the k_{cat} values of misaminoacylation normalized to the respective values of phenylalanylation vary from 1.5 for *Hsmt*PheRS to 6.7 for *Tt*PheRS. The $K_m^{L\text{-dopa}}/K_m^{Phe}$ ratios are quite similar for all PheRSs (range from 200 to 230). The observed resemblance of *Hsmt*PheRS and *Tt*PheRS in the binding discrimination is consistent with structural data showing closely similar architectures of the amino acid binding pockets of two proteins.

Binding of Levodopa in the Editing Site

In the complex of *Tt*PheRS with L-dopa a second molecule of the ligand was identified at the interface between B3 and B4 domains of the αβ heterodimer. A clear and strong electron density (>3.0 σ) on the (F_{obs}-F_{calc}) map (Figure 1B) may be unambiguously attributed to the L-dopa molecule. As it was revealed previously, the distinct pocket visualized on the β subunit is most likely related to the editing activity of bacterial PheRSs (Kotik-Kogan et al., 2005; Roy et al., 2004). The editing site in bacterial PheRSs is designed for anchoring L-Tyr attached to the tRNA^{Phe}, and for subsequent hydrolysis of misacylated tRNA^{Phe}. The phenyl ring of Pheβ360 and the side chain of Proβ259 provide edge-to-face interactions with the L-Tyr moiety. Pheβ360 is strictly conserved in eubacterial PheRSs, whereas Proβ259 is replaced in a few cases with Ile or Leu capable of participating in hydrophobic interactions. The net of hydrogen bonding between L-Tyr and side chains of amino acids lining the interior within the editing site was described before, among which the interactions

Table 2. Kinetic Constants of tRNA^{Phe} Aminoacylation

PheRS	Amino acid	K_m(μM)	k_{cat}(min^{-1})	k_{cat}/K_m(μM^{-1} min^{-1})	k_{cat}/K_m(relative)[c]	K_i^{app}(μM)
*Tt*PheRS	Phe[a,e]	1.8 ± 0.2	65 ± 3	36 ± 4		
	Phe[a]	1.7 ± 0.3[d]	67 ± 4[d]	39 ± 7	1.0	
	Tyr[a,e]					3100 ± 300
	m-Tyr[a,e]					13.0 ± 0.4
	L-dopa[a]	380 ± 40[d]	9.7 ± 0.5[d]	0.026 ± 0.004	0.00065	
*Hsct*PheRS	Phe[b]	3.2 ± 0.4[d]	52 ± 3[d]	16 ± 3	1.0	
	Tyr[e]					3400 ± 400
	m-Tyr[b]	130 ± 20[d]	39 ± 2[d]	0.30 ± 0.06	0.019	150 ± 10
	L-dopa[b]	650 ± 100[d]	14 ± 1[d]	0.022 ± 0.004	0.0013	
*Hsmt*PheRS	Phe[a,e]	2.2 ± 0.4[d]	2.6 ± 0.4[d]	1.2 ± 0.2	1.0[a]	
	Phe[b]	2.6 ± 0.3[d]	4.5 ± 0.3[d]	1.7 ± 0.3	1.0[b]	
	Tyr[a,e]	1900 ± 300[d]	2.0 ± 0.2[d]	0.0010 ± 0.0002	0.00089	
	m-Tyr[a,e]	12 ± 1[d]	3.1 ± 0.2[d]	0.26 ± 0.04	0.22	13.6 ± 0.7
	L-dopa[a]	520 ± 90[d]	1.6 ± 0.1[d]	0.0031 ± 0.0006	0.0026	
	L-dopa[b]	600 ± 100[d]	3.4 ± 0.2[d]	0.0057 ± 0.0009	0.0033	

[a] *E. coli* tRNA^{Phe}-transcript was used in the experiments with *Tt*PheRS or *Hsmt*PheRS.
[b] Human cytoplasmic tRNA^{Phe}-transcript was used in kinetic measurements for *Hsct*PheRS or *Hsmt*PheRS.
[c] Relative k_{cat}/K_m values are normalized for each PheRS and tRNA^{Phe} to the corresponding value for phenylalanine.
[d] Values obtained from the acid gel electrophoresis technique; the other data presented were determined by the tRNA precipitation assay. Data are presented as means of at least three independent experiments with standard deviation of the mean.
[e] Data taken from our previous work (Klipcan et al., 2009).

between the Tyr OH group in *para*-position and the O$^{\varepsilon 1}$ of Gluβ334 and the main chain amide of Glyβ315 are the most important (Kotik-Kogan et al., 2005). Binding mode of L-dopa in this area is characterized by appearance of the extra hydrogen bonds, as compared to L-Tyr, formed also by the OH group in *meta*-position of the aromatic moiety with the O$^{\varepsilon 2}$ of Gluβ334 and the main chain amide of Glyβ315. Thus, the carboxylic group of Gluβ334 makes direct hydrogen bonds with two OH groups of 3,4-dihydroxy-L-phenylalanine.

Trans Editing of L-Dopa-tRNA^{Phe} by PheRS

Detection of L-dopa in the editing site of *Tt*PheRS prompted us to investigate the hydrolytic activity of the enzyme toward L-dopa-tRNA^{Phe}. The mischarged product was presynthesized in the presence of *Hsmt*PheRS, isolated from the reaction mixture, and then incubated in the presence of varied concentrations of *Tt*PheRS (Figure 3A). The enzyme catalyzes hydrolysis of exogenous L-dopa-tRNA^{Phe}. The rate of hydrolysis depends on the enzyme concentration and even at the lowest concentration tested is significantly higher than the rate of spontaneous deacylation (compare lanes 1–3 and lanes 10–14, Figure 3A). The apparent rate constants estimated from the kinetic data are 0.27 min^{-1} for the enzyme-assisted hydrolysis (at 16 nM *Tt*PheRS) and 0.04 min^{-1} for the spontaneous degradation. Addition of L-dopa to the reaction mixture revealed no effect of the free amino acid on the editing activity, suggesting that there is no competition between the editing substrate and L-dopa for binding in the hydrolytic active site (compare lanes 1–3, 7–9, and lanes 15–20, Figure 3A). However, incubation of L-dopa-tRNA^{Phe} under hydrolysis conditions in the presence of *Tt*PheRS, L-dopa, and ATP showed a new stable level of the aminoacylation product, which depends on both the amino acid (see lanes 22–24 and 28–30, Figure 3A) and enzyme concentration (not shown). The observed level is evidently due to reaminoacylation of the deacylated tRNA^{Phe} and reflects the balance between the two enzymatic reactions. Indeed, the enzymatic hydrolysis occurred normally (with the same efficiency as in the absence of small substrates) when L-dopa and ATP were added simultaneously with PheOH-AMP, a stable synthetic analog of phenylalanyl-adenylate. Binding of this strong competitive inhibitor in the aminoacylation active site of *Tt*PheRS completely suppressed reaminoacylation of the deacylated tRNA. The data indicate that *Tt*PheRS is active in editing of L-dopa-tRNA^{Phe} in *trans*, i.e., after dissociation of the mischarged product from the aminoacylation complex and further rebinding.

Hydrolysis experiments with Tyr-tRNA^{Phe} (Figure 3B) revealed that *Tt*PheRS edits Tyr-tRNA^{Phe} and L-dopa-tRNA^{Phe} in *trans* with closely similar efficiencies (compare lanes 4–9, Figure 3A, and lanes 6–11, Figure 3B). Moreover, Tyr-tRNA^{Phe} is also reaminoacylated with L-dopa; the reaction occurs with the same efficiency as in the case of L-dopa-tRNA^{Phe}, and it is completely inhibited in the presence of PheOH-AMP (lanes 12–20, Figure 3B). To compare *trans*-editing activities of *Tt*PheRS toward L-dopa-tRNA^{Phe} and Tyr-tRNA^{Phe}, we performed additional kinetic experiments using a standard tRNA precipitation assay. The presynthesized nonradiolabeled Tyr-tRNA^{Phe} and L-dopa-tRNA^{Phe} were incubated under the hydrolysis conditions in the presence of *Tt*PheRS, [^{3}H]phenylalanine and ATP, and incorporation of the radioactive amino acid into tRNA was measured (Figure 4). The relative amount of the deacylated form in the aa-tRNA preparations (accumulated during isolation and purification) was checked in control experiments with *Hsmt*PheRS, which has no editing activity. The concentrations of enzymes were adjusted in the control experiments (not shown) to ensure

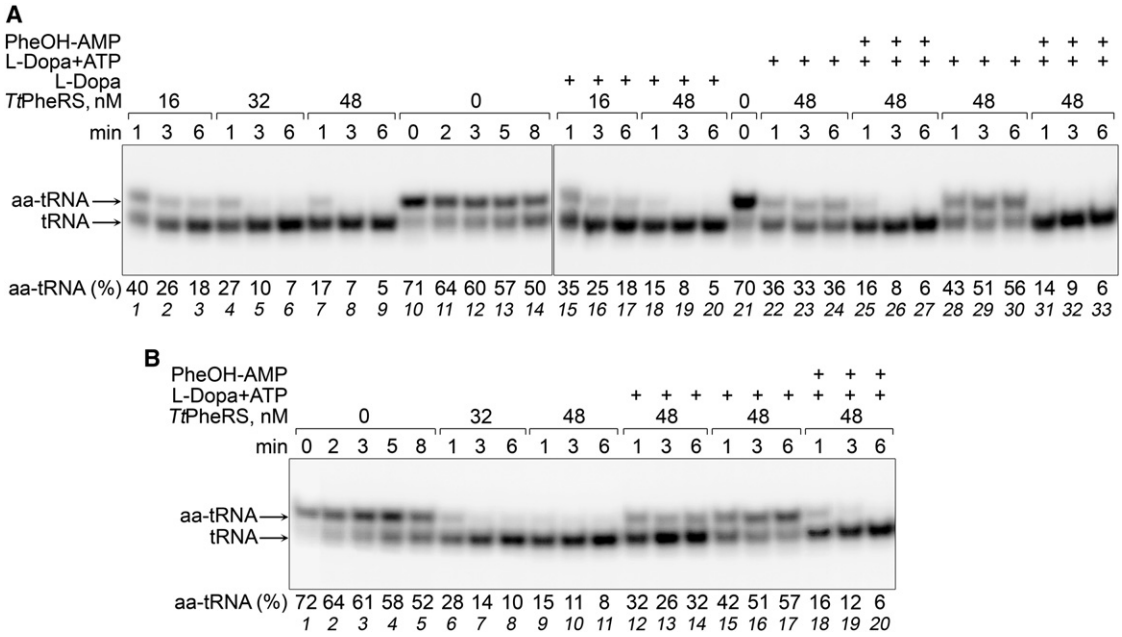

Figure 3. Specific Hydrolysis of Misacylated tRNA^{Phe}s by *Tt*PheRS

Hydrolysis of (A) 1 μM L-dopa-tRNA^{Phe} and (B) 1 μM Tyr-tRNA^{Phe} in absence or presence of varied *Tt*PheRS concentrations. The mischarged aa-tRNAs were presynthesized from ^{32}P-labeled *Ec*tRNA^{Phe} (using *Hsmt*PheRS) and purified. The enzyme-catalyzed hydrolysis was initiated after 2 min of preincubation. When indicated 2 mM (A, lanes 15–20 and 28–33; B, lanes 15–20) or 400 μM L-dopa (A, lanes 22–27; B, lanes 12–14)], 2 mM ATP and 150 μM PheOH-AMP were added to the reaction mixture. The charging level of tRNA was analyzed by electrophoresis in 8% denaturing gel at acidic conditions. Gels are representative images from three independent experiments. See also Figure S1A.

full charging of free tRNA^{Phe} after 1.5–2 min of incubation. The charging level in the presence of *Hsmt*PheRS after 2 min of incubation (~30%) corresponds to the content of free tRNA (determined independently by the acidic gel electrophoresis) in the presynthesized aa-tRNA preparations. The further slow increase of the charging level (up to 55%) in the presence of *Hsmt*PheRS is caused by phenylalanylation of the aa-tRNA spontaneously degraded during the incubation. The reaction in the presence of *Tt*PheRS shows that both Tyr-tRNA^{Phe} and L-dopa-tRNA^{Phe} are completely recharged within the incubation time, with the initial reaction rates being practically identical. These data provide further evidence of close similarity of the two misacylated tRNA^{Phe}s as *trans*-editing substrates of *Tt*PheRS.

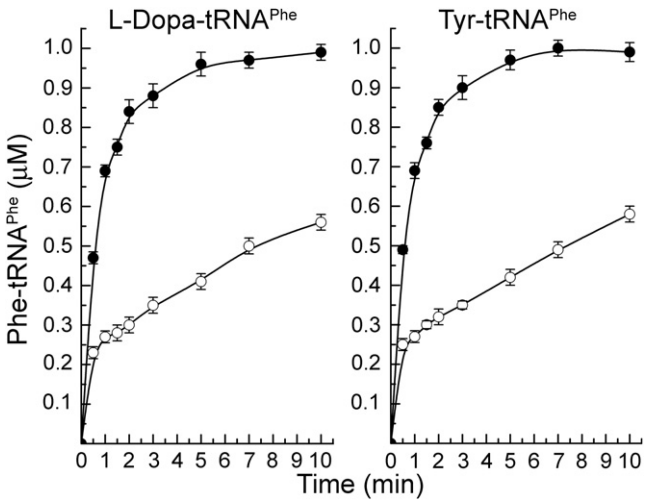

Figure 4. Comparison of *Tt*PheRS Hydrolytic Activities toward L-Dopa-tRNA^{Phe} and Tyr-tRNA^{Phe} by Reaminoacylation Assay

The nonradiolabeled *Ec*tRNA^{Phe} was preaminoacylated with L-dopa or Tyr and purified, then incubated (at 1 μM concentration) in the hydrolysis reaction mixture in the presence of ATP, [^{3}H]Phe, and *Tt*PheRS (filled symbols) or *Hsmt*PheRS (open symbols). Values shown are the means of three independent experiments with standard deviation of the mean. See also Figure S1B.

Trans-editing activity toward L-dopa-tRNA^{Phe} was also investigated for *Hsct*PheRS (see Figure S1A available online). The exogenous mischarged product was efficiently hydrolyzed by the enzyme in the absence of L-dopa and ATP, or when the small substrates were added simultaneously with PheOH-AMP, which inhibited completely the aminoacylation reaction. *Trans*-editing activities of *Hsct*PheRS toward L-dopa-tRNA^{Phe} and Tyr-tRNA^{Phe} were compared by kinetic measurements of [^{3}H] phenylalanine incorporation into the presynthesized nonradiolabeled aa-tRNA^{Phe}s (Figure S1B). The observed rates of reaminoacylation indicate that *Hsct*PheRS hydrolyzes L-dopa-tRNA^{Phe} and Tyr-tRNA^{Phe} in *trans* with very similar efficiencies. Thus, editing activity toward L-dopa-tRNA^{Phe} is a common characteristic of bacterial and eukaryotic cytoplasmic PheRSs.

The aminoacylation and hydrolysis data taken together show the discrimination between Phe and L-dopa by *Tt*PheRS and *Hsct*PheRS to relay on a complicated multistep process. The k_{cat} values of L-dopa-tRNA^{Phe} synthesis by these enzymes presented in Table 2 should be considered as apparent rate

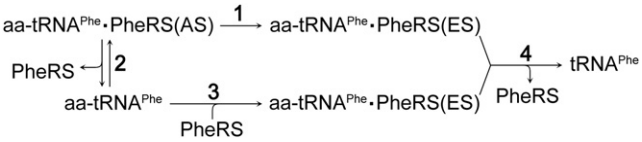

Figure 5. Scheme of Editing Pathways

Cis-editing pathway consists of steps 1 and 4: synthesized in the aminoacylation active site (AS) misacylated tRNA (aa-tRNA^{Phe}) translocates to the editing site (ES) within the complex with PheRS and is hydrolyzed. *Trans*-editing pathway consists of steps 2, 3, and 4: mischarged product dissociates from the complex with PheRS, rebinds to the editing site and than is hydrolyzed.

constants, because they reflect the overall rates of misaminoacylation, which depend on the ratio of the rates of formation and further hydrolysis. Therefore, the observed difference between three PheRSs in the discrimination efficiencies at the level of k_{cat} values may result from differences in the true rate constant for aa-tRNA formation and in the contribution of editing reaction to the overall yield of the mischarged product.

DISCUSSION

A number of studies have shown that ROS-damaged amino acids, *m*-Tyr, *o*-Tyr, and L-dopa, are incorporated in vitro and in vivo into proteins alongside with the canonical amino acids via the translational apparatus of bacterial and eukaryotic cells (Rodgers and Shiozawa, 2008). However, the particular molecular pathways of oxidized amino acids translation and specifically the role of aaRSs in this process are far from being completely understood. L-Dopa has been shown to be incorporated into nascent proteins by bacterial and mammalian cells (Rodgers and Shiozawa, 2008) and has been detected before to act as a substrate of bacterial TyrRS (Calendar and Berg, 1966). Recently we have revealed that *m*-Tyr may be incorporated into eukaryotic proteins, using mitochondrial and cytoplasmic PheRSs (Klipcan et al., 2009). The present study is the first evidence that all three major forms of PheRS (mitochondrial and cytoplasmic eukaryotic, and bacterial) catalyze mischarging of tRNA^{Phe} with L-dopa, thereby opening the way for translational incorporation of the oxidized tyrosine analog in place of phenylalanine.

The aminoacylation kinetic experiments with *Hsmt*PheRS, *Hsct*PheRS, and *Tt*PheRS revealed that all the enzymes display relative specificity constants for L-dopa over Phe substrate in the range 3×10^{-3}–6×10^{-4} (as reflected in relative k_{cat}/K_m values; see Table 2). These values significantly exceed the error rates in protein translation estimated to be $<10^{-4}$ (Hendrickson et al., 2004). The overall error rate of aa-tRNA synthesis is determined by both aaRS specificity and the relative concentrations of the cognate and noncognate substrates in the cell. Given that mitochondrial respiration is a major source of ROS and oxidized amino acids (Winterbourn, 2008), and *Hsmt*PheRS displays the lowest level of discrimination against L-dopa, we hypothesize the leading role of this enzyme in misincorporation of L-dopa into proteins, opening up the way for delivery of the misacylated tRNA to the ribosome. Moreover, the relative specificity constant of TyrRS for L-dopa over the cognate amino acid ($\sim 5 \times 10^{-3}$), reported only for the bacterial enzyme (Calendar and Berg, 1966), is comparable to that of *Hsmt*PheRS, suggesting competition of two enzymes for L-dopa upon its attachment to tRNA and further misincorporation into proteins. In view of our findings, engineered tRNA-PheRS pairs seem to be perspective (alternative to tRNA-TyrRS pairs) tools for selective incorporation of the redox-active amino acid into proteins, which in turn offers new opportunities to study impact of physiologically relevant protein modifications on cell function.

All three PheRSs discriminate L-dopa less efficiently than Tyr at the binding level, as is evident from comparison of the respective K_m (or K_m and K_i) values (see Table 2). Their higher affinity for L-dopa is consistent with structural data: the position of L-dopa within the aminoacylation active site is additionally stabilized by hydrogen bonding of the OH-group in *meta*-position. Like Tyr, L-dopa is bound in the editing site of *Tt*PheRS. Moreover, both *Tt*PheRS and *Hsct*PheRS catalyze hydrolysis of exogenous L-dopa-tRNA^{Phe} and Tyr-tRNA^{Phe} with similar efficiencies. These data suggest that PheRS editing activity in *trans*, i.e., through rebinding and hydrolysis of misacylated tRNA^{Phe} released to solution (Figure 5), is practically insensitive to structural differences between L-dopa and Tyr. As shown by fast kinetic study of yeast PheRS (Lin et al., 1984), Tyr-tRNA^{Phe} (never detected by steady-state aminoacylation kinetics) is only transiently formed with the rate constant, which is 11-fold lower than the respective hydrolysis rate constant. The observed accumulation of L-dopa-tRNA^{Phe} under steady-state aminoacylation conditions indicates that the rate constant of its formation exceeds the hydrolysis rate constant. Different rations between the hydrolysis and aminoacylation rate constants may result from more efficient synthesis of L-dopa-tRNA^{Phe} compared to that of Tyr-tRNA^{Phe}. A comparative kinetic study of tRNA^{Phe} tyrosylation by editing-defective PheRS will be helpful. Alternative hypothesis is that L-dopa-tRNA^{Phe} is less efficiently hydrolyzed than Tyr-tRNA^{Phe} through the *cis*-editing pathway, i.e., by translocation to the editing site within the complex with PheRS. Little is known about the mechanism of translocation of incorrect product from the aminoacylation to the editing site. Based on structural and modeling studies, it is generally believed that the tRNA acceptor end acylated with the noncognate amino acid shuttles between the two sites (as a result of a conformational change), whereas the tRNA body is still bound to the aaRS (Dock-Bregeon et al., 2000; Fukunaga and Yokoyama, 2005; Silvian et al., 1999; Tukalo et al., 2005). In the present state of knowledge, influence of the amino acid structure on the efficiency of translocation cannot be excluded. The recognition of tRNA^{Phe} during *trans* editing was investigated by mutagenesis (Ling et al., 2009). G34, the major identity element of tRNA^{Phe} aminoacylation, is less efficiently (by 2–7-fold) recognized by the wild-type and mutant PheRSs during editing than during aminoacylation, indicating that PheRS interactions with the anticodon are not completely conserved in the *trans*-editing complex. The relative contributions of *cis*- and *trans*-editing pathways to the proofreading are yet unknown. Previous observations of Tyr mistranslation at Phe codons resulted from coexpressing wild-type and editing-defective PheRSs (Roy et al., 2004) indicate that the *trans*-editing activity is ineffective to reduce the aminoacylation error rate. At the step following the aminoacylation, no discrimination between Tyr-tRNA^{Phe} and Phe-tRNA^{Phe} by the elongation factor EF-Tu was detected

(Ling et al., 2009). However, PheRS was shown to rebind and edit the mischarged tRNA in the presence of EF-Tu, thus leading to a reduction in the overall error rate of aminoacylation. This additional editing step prior to translocation to the ribosome cannot be excluded for L-dopa-tRNA^{Phe}, based on its similarity to Tyr-tRNA^{Phe} in the *trans* editing.

SIGNIFICANCE

Protein-bound L-dopa is one of the prevailing ROS-damaged modifications of amino acids identified in tissue proteins of atherosclerotic plaques (Fu et al., 1998a, 1998b) and cataract lens (Molnár et al., 2005). Unlike some other oxidized amino acids, L-dopa is a reactive species further oxidized to dopaquinone, readily forming covalent links with other species and generating products such as 5-S-cysteinyldopa capable of crosslinking proteins (Rodgers and Dean, 2000). This in turn may create proteins resistant to proteolysis and forming stable aggregates preventing their efficient removal (Davies, 2001; Kopito, 2000). Although considerable information has accumulated on incorporation of ROS-damaged amino acids into proteins and their impact on cell functions and associated diseases, very little is known about the particular pathways of discrimination and misincorporation of these specific compounds. Here, we provide for the first time structural and kinetic data on interaction of three structurally different wild-type forms of PheRS with L-dopa. The relative specificity constants for L-dopa over Phe in the aminoacylation reaction identify the bacterial and eukaryotic PheRSs as potential contributors to biosynthesis of L-dopa containing proteins. Recent study of oxidized proteins catabolism (Dunlop et al., 2011) revealed that L-dopa-containing proteins are more potent inducers of apoptosis than proteins containing *ortho*-tyrosine. The observed effects upon the oxidized amino acids incorporation into polypeptide chains may associate with inability of human and bacterial PheRSs to catalyze tRNA^{Phe} mischarging with *o*-Tyr (our unpublished results). Protein-bound L-dopa may play important role in progression of age-related disorders by contributing to lysosomal membrane permeabilization-initiated apoptosis and may have important implications for the long-term use of L-dopa as a therapeutic agent in Parkinson's disease (Dunlop et al., 2011). Protection against misincorporation of oxidative-damaged amino acids could constitute a promising approach to the treatment of ROS-dependent pathologies.

EXPERIMENTAL PROCEDURES

Chemicals, Proteins, and tRNAs

3,4-Dihydroxy-L-phenylalanine, DL-*m*-tyrosine, L-*p*-tyrosine, and L-phenylalanine were purchased from Sigma-Aldrich, L-[^{3}H]phenylalanine was from Amersham Biosciences. Phenylalaninyl-5′-adenylate (PheOH-AMP) was synthesized and purified as described (Cassio et al., 1967). The tRNA^{Phe}s (*E. coli* and human cytoplasmic) were synthesized by using runoff transcription of synthetic genes with T7 RNA polymerase followed by electrophoretic isolation of the correct-length transcripts as described (Vasil'eva et al., 2002). To prepare the ^{32}P-labeled tRNAs, transcriptions were run in the presence of α-[^{32}P]ATP (Amersham Biosciences). Phenylalanyl-tRNA synthetases were purified from natural (*Tt*PheRS) or overexpressed sources (*Hsct*PheRS and *Hsmt*PheRS) as described (Chernaya et al., 1987; Levin et al., 2007; Moor et al., 2002).

tRNA Aminoacylation

Aminoacylation reaction was performed in conditions optimized for tRNA phenylalanylation by different PheRSs (Moor et al., 2002; Vasil'eva et al., 2002). The activity of *Hsct*PheRS was tested generally at 30°C in reaction mixtures containing 50 mM tris-HCl, pH 8.0, 30 mM $MgCl_2$, 20 mM KCl, 5 mM dithiothreitol (DTT), 5 mM ATP, and 2–2.8 μM *Hs*tRNA^{Phe}-transcript. In experiments with *Tt*PheRS and *Hsmt*PheRS performed at 37°C the reaction mixtures contained 50 mM tris-HCl, pH 8.5, 15 mM $MgCl_2$ (or 9 mM $MgCl_2$ for aminoacylation of *Ec*tRNA^{Phe} by *Tt*PheRS), 5 mM DTT, 5 mM ATP, and 1.3–4 μM *Ec*tRNA^{Phe}-transcript or 2–3 μM *Hs*tRNA^{Phe}-transcript. Both *Ec*tRNA^{Phe}-transcript and *Hs*tRNA^{Phe}-transcript are heterologous substrates of *Tt*PheRS and *Hsmt*PheRS, which can be efficiently aminoacylated in definite conditions. The amino acid concentrations varied from 200 nM to 40 μM for Phe, from 10 μM to 2 mM for *m*-Tyr, and from 100 μM to 3.4 mM for L-dopa. Aminoacylation of ^{32}P-labeled tRNA^{Phe} with unlabeled cognate and noncognate amino acids was tested by an acidic gel electrophoretic method (Varshney et al., 1991). Aliquots (4 μL) of reaction solution were quenched at various time points in 6 μl of loading solution containing 0.1 M sodium acetate (pH 5), 7 M urea, and leading dyes. Gels were run at 4°C for 15 hr at 6 V/cm for a 12-cm migration of xylene cyanol, dried, and quantified by Phosphor imaging. The level of spontaneous deacylation during electrophoresis, which was checked by comparative measurement of the aminoacylation extent in identical conditions by using the trichloroacetic acid precipitation assay and ^{14}C/^{3}H-labeled Phe, did not exceed 15%. The kinetic parameters were calculated by a nonlinear regression fit of the data to a Michaelis-Menten equation. The reported k_{cat} and K_m values are the means of at least three independent experiments with standard deviations indicated.

Preparative Synthesis of aa-tRNA^{Phe} and Posttransfer Editing Assay

Aminoacylation of 4 μM ^{32}P-labeled tRNA^{Phe}-transcript (*Ec*tRNA^{Phe} or *Hs*tRNA^{Phe}) with phenylalanine or noncognate amino acids was performed in the presence of a sub-saturating concentration of the amino acid (50 μM Phe, 200 μM *m*-Tyr, 1.7 mM Tyr, or 3.4 mM L-dopa) and definite concentration of *Hsmt*PheRS (0.4 μM for charging with Phe or *m*-Tyr; 1.6 μM for charging with L-dopa; 3.2 μM for tyrosylation). After 30 min of incubation at 37°C in the mixtures containing all the other components described above for tRNA aminoacylation, the reaction was stopped by addition of four volumes of cold solution of 300 mM sodium acetate (pH 4.9). The remaining ATP and amino acid were separated by exhaustive dialysis at 4°C against 300 mM sodium acetate (pH 4.9), containing 15 mM $MgCl_2$ and 5 mM DTT, using Vivaspin microconcentrator. The aa-tRNA was extracted with phenol (buffered with 100 mM sodium acetate, pH 4.9), followed by chloroform extraction, ethanol precipitation and stepwise washing with 70% and absolute ethanol. The aa-tRNA pellet was dried, stored at −20°C and dissolved in water directly before hydrolysis experiments. The aa-tRNA yields were within the range 70%–80%.

The hydrolysis reaction mixtures contained 50 mM tris-HCl, pH 8.0, 20 mM $MgCl_2$, 1 μM ^{32}P-labeled aa-tRNA^{Phe}. When indicated, the reaction mixture contained L-dopa, ATP, and PheOH-AMP. The mixture was preincubated for 2 min at 37°C, and the editing reaction initiated by addition of *Tt*PheRS (16–48 nM) or *Hsct*PheRS (20–60 nM) was followed by measuring the extent of charged tRNA in the aliquots by the acidic gel electrophoretic method described above.

Posttransfer editing was also assayed by reaminoacylation of L-dopa-tRNA^{Phe} and Tyr-tRNA^{Phe} with L-[^{3}H]Phe. The nonradiolabeled aa-tRNA (0.8–1 μM) synthesized and purified as described above was incubated at 37°C in the hydrolysis reaction mixture in the presence of 5 mM ATP, 4 μM L-[^{3}H]Phe, and 60 nM *Tt*PheRS, or 200 nM *Hsmt*PheRS, or 90 nM *Hsct*PheRS. The enzyme concentrations have been adjusted in the control experiments to ensure full aminoacylation of 1 μM uncharged tRNA^{Phe}-transcript after 1.5–3 min of incubation. At the appropriate times aliquots of 6 μl were spotted onto Whatman filter paper impregnated with 5% trichloroacetic acid (TCA). Then the filters were extensively washed with ice-cold 5% TCA, and TCA-insoluble radioactivity was measured by liquid scintillation counting.

Crystallization and Structure Determination

Crystallization of *Tt*PheRS and *Hsmt*PheRS with various ligands has been described in detail (Chernaya et al., 1987; Kotik-Kogan et al., 2005; Levin et al., 2007). Crystal soaking with L-dopa for *Tt*PheRS and *Hsmt*PheRS was carried out under conditions similar to those described. Along with other components 5 mM DTT was added to the soaking solutions. Complete X-ray datasets were collected from single crystals at European Synchrotron Radiation Facility BM-14 station. The structures of *Tt*PheRS and *Hsmt*PheRS complexed with L-dopa were isomorphous to the native ones. After rigid-body refinement (REFMAC5) and cycles of simulated annealing and conjugate gradient minimization (CNS), an unbiased difference Fourier map with coefficients (F_{obs}-F_{calc}) was calculated (Brünger et al., 1998; Murshudov et al., 1997). Water molecules were added by using Arp/Warp (Jones et al., 1991). The manual refinement of the model building was done with O and Coot (Emsley and Cowtan, 2004; Jones et al., 1991). The models were refined to R_{work}/R_{free} of 17%/22% and 23%/29% for *Hsmt*PheRS and *Tt*PheRS, respectively.

ACCESSION NUMBERS

Atomic coordinates and structure factors for *Hsmt*PheRS and *Tt*PheRS complexes with L-dopa have been deposited in the Protein Data Bank under codes 3TEG and 3TEH, respectively.

SUPPLEMENTAL INFORMATION

Supplemental Information includes one figure and can be found with this article online at doi:10.1016/j.chembiol.2011.08.008.

ACKNOWLEDGMENTS

This work was supported by Israel Science Foundation (grant 710262 to M.S.), by the Kimmelman Center for Biomolecular Structure and Assembly at Weizmann Institute of Science (M.S.), Russian Foundation of Basic Research (grant 10-04-01082 to N.M.), Siberian Branch of RAS (interdisciplinary grant 13 to N.M.), and the Ori Foundation doctoral research fellowship (L.K.). M.S. holds the Lee & William Abramowitz Professorial Chair of Molecular Biophysics.

Received: June 22, 2011
Revised: August 5, 2011
Accepted: August 8, 2011
Published: October 27, 2011

REFERENCES

Alfonta, L., Zhang, Z., Uryu, S., Loo, J.A., and Schultz, P.G. (2003). Site-specific incorporation of a redox-active amino acid into proteins. J. Am. Chem. Soc. *125*, 14662–14663.

Brünger, A.T., Adams, P.D., Clore, G.M., DeLano, W.L., Gros, P., Grosse-Kunstleve, R.W., Jiang, J.S., Kuszewski, J., Nilges, M., Pannu, N.S., et al. (1998). Crystallography & NMR system: a new software suite for macromolecular structure determination. Acta Crystallogr. D Biol. Crystallogr. *54*, 905–921.

Burdine, L., Gillette, T.G., Lin, H.J., and Kodadek, T. (2004). Periodate-triggered cross-linking of DOPA-containing peptide-protein complexes. J. Am. Chem. Soc. *126*, 11442–11443.

Calendar, R., and Berg, P. (1966). The catalytic properties of tyrosyl ribonucleic acid synthetases from *Escherichia coli* and *Bacillus subtilis*. Biochemistry *5*, 1690–1695.

Cassio, D., Lemoine, F., Waller, J.P., Sandrin, E., and Boissonnas, R.A. (1967). Selective inhibition of aminoacyl ribonucleic acid synthetases by aminoalkyl adenylates. Biochemistry *6*, 827–836.

Chernaya, M.M., Korolev, S.V., Reshetnikova, L.S., and Safro, M.G. (1987). Preliminary crystallographic study of the phenylalanyl-tRNA synthetase from *Thermus thermophilus* HB8. J. Mol. Biol. *198*, 555–556.

Davies, K.J. (2001). Degradation of oxidized proteins by the 20S proteasome. Biochimie *83*, 301–310.

Dock-Bregeon, A., Sankaranarayanan, R., Romby, P., Caillet, J., Springer, M., Rees, B., Francklyn, C.S., Ehresmann, C., and Moras, D. (2000). Transfer RNA-mediated editing in threonyl-tRNA synthetase. The class II solution to the double discrimination problem. Cell *103*, 877–884.

Dunlop, R.A., Brunk, U.T., and Rodgers, K.J. (2011). Proteins containing oxidized amino acids induce apoptosis in human monocytes. Biochem. J. *435*, 207–216.

Emsley, P., and Cowtan, K. (2004). Coot: model-building tools for molecular graphics. Acta Crystallogr. D Biol. Crystallogr. *60*, 2126–2132.

Fishman, R., Ankilova, V., Moor, N., and Safro, M. (2001). Structure at 2.6 A resolution of phenylalanyl-tRNA synthetase complexed with phenylalanyl-adenylate in the presence of manganese. Acta Crystallogr. D Biol. Crystallogr. *57*, 1534–1544.

Fu, S., Davies, M.J., Stocker, R., and Dean, R.T. (1998a). Evidence for roles of radicals in protein oxidation in advanced human atherosclerotic plaque. Biochem. J. *333*, 519–525.

Fu, S., Dean, R., Southan, M., and Truscott, R. (1998b). The hydroxyl radical in lens nuclear cataractogenesis. J. Biol. Chem. *273*, 28603–28609.

Fukunaga, R., and Yokoyama, S. (2005). Aminoacylation complex structures of leucyl-tRNA synthetase and tRNA^{Leu} reveal two modes of discriminator-base recognition. Nat. Struct. Mol. Biol. *12*, 915–922.

Hendrickson, T.L., de Crécy-Lagard, V., and Schimmel, P. (2004). Incorporation of nonnatural amino acids into proteins. Annu. Rev. Biochem. *73*, 147–176.

Jones, T.A., Zou, J.Y., Cowan, S.W., and Kjeldgaard, M. (1991). Improved methods for building protein models in electron density maps and the location of errors in these models. Acta Crystallogr. A *47*, 110–119.

Klipcan, L., Moor, N., Kessler, N., and Safro, M.G. (2009). Eukaryotic cytosolic and mitochondrial phenylalanyl-tRNA synthetases catalyze the charging of tRNA with the *meta*-tyrosine. Proc. Natl. Acad. Sci. USA *106*, 11045–11048.

Kopito, R.R. (2000). Aggresomes, inclusion bodies and protein aggregation. Trends Cell Biol. *10*, 524–530.

Kotik-Kogan, O., Moor, N., Tworowski, D., and Safro, M. (2005). Structural basis for discrimination of L-phenylalanine from L-tyrosine by phenylalanyl-tRNA synthetase. Structure *13*, 1799–1807.

Levin, I., Kessler, N., Moor, N., Klipcan, L., Koc, E., Templeton, P., Spremulli, L., and Safro, M. (2007). Purification, crystallization and preliminary X-ray characterization of a human mitochondrial phenylalanyl-tRNA synthetase. Acta Crystallogr. Sect. F Struct. Biol. Cryst. Commun. *63*, 761–764.

Lin, S.X., Baltzinger, M., and Remy, P. (1984). Fast kinetic study of yeast phenylalanyl-tRNA synthetase: role of tRNA^{Phe} in the discrimination between tyrosine and phenylalanine. Biochemistry *23*, 4109–4116.

Ling, J., So, B.R., Yadavalli, S.S., Roy, H., Shoji, S., Fredrick, K., Musier-Forsyth, K., and Ibba, M. (2009). Resampling and editing of mischarged tRNA prior to translation elongation. Mol. Cell *33*, 654–660.

Molnár, G.A., Nemes, V., Biró, Z., Ludány, A., Wagner, Z., and Wittmann, I. (2005). Accumulation of the hydroxyl free radical markers *meta*-, *ortho*-tyrosine and DOPA in cataractous lenses is accompanied by a lower protein and phenylalanine content of the water-soluble phase. Free Radic. Res. *39*, 1359–1366.

Moor, N., Linshiz, G., and Safro, M. (2002). Cloning and expression of human phenylalanyl-tRNA synthetase in *Escherichia coli*: comparative study of purified recombinant enzymes. Protein Expr. Purif. *24*, 260–267.

Murshudov, G.N., Vagin, A.A., and Dodson, E.J. (1997). Refinement of macromolecular structures by the maximum-likelihood method. Acta Crystallogr. D Biol. Crystallogr. *53*, 240–255.

Ozawa, K., Headlam, M.J., Mouradov, D., Watt, S.J., Beck, J.L., Rodgers, K.J., Dean, R.T., Huber, T., Otting, G., and Dixon, N.E. (2005). Translational incorporation of L-3,4-dihydroxyphenylalanine into proteins. FEBS J. *272*, 3162–3171.

Reshetnikova, L., Moor, N., Lavrik, O., and Vassylyev, D.G. (1999). Crystal structures of phenylalanyl-tRNA synthetase complexed with phenylalanine and a phenylalanyl-adenylate analogue. J. Mol. Biol. *287*, 555–568.

Rodgers, K.J., and Dean, R.T. (2000). Metabolism of protein-bound DOPA in mammals. Int. J. Biochem. Cell Biol. *32*, 945–955.

Rodgers, K.J., and Shiozawa, N. (2008). Misincorporation of amino acid analogues into proteins by biosynthesis. Int. J. Biochem. Cell Biol. *40*, 1452–1466.

Roy, H., Ling, J., Alfonzo, J., and Ibba, M. (2005). Loss of editing activity during the evolution of mitochondrial phenylalanyl-tRNA synthetase. J. Biol. Chem. *280*, 38186–38192.

Roy, H., Ling, J., Irnov, M., and Ibba, M. (2004). Post-transfer editing *in vitro* and *in vivo* by the beta subunit of phenylalanyl-tRNA synthetase. EMBO J. *23*, 4639–4648.

Silvian, L.F., Wang, J., and Steitz, T.A. (1999). Insights into editing from an ile-tRNA synthetase structure with tRNA^{ile} and mupirocin. Science *285*, 1074–1077.

Tukalo, M., Yaremchuk, A., Fukunaga, R., Yokoyama, S., and Cusack, S. (2005). The crystal structure of leucyl-tRNA synthetase complexed with tRNA^{Leu} in the post-transfer-editing conformation. Nat. Struct. Mol. Biol. *12*, 923–930.

Umeda, A., Thibodeaux, G.N., Zhu, J., Lee, Y., and Zhang, Z.J. (2009). Site-specific protein cross-linking with genetically incorporated 3,4-dihydroxy-L-phenylalanine. ChemBioChem *10*, 1302–1304.

Varshney, U., Lee, C.P., Seong, B.L., and RajBhandary, U.L. (1991). Mutants of initiator tRNA that function both as initiators and elongators. J. Biol. Chem. *266*, 18018–18024.

Vasil'eva, I.A., Ankilova, V.N., Lavrik, O.I., and Moor, N.A. (2002). tRNA discrimination by *T. thermophilus* phenylalanyl-tRNA synthetase at the binding step. J. Mol. Recognit. *15*, 188–196.

Winterbourn, C.C. (2008). Reconciling the chemistry and biology of reactive oxygen species. Nat. Chem. Biol. *4*, 278–286.